FOUNDATIONS
ADVANCES

Volume 72 (2016)

Supporting information for article:

Towards atomistic understanding of polymorphism in the solvothermal synthesis of ZrO2 nanoparticles

Ann-Christin Dippel, Kirsten M. Ø. Jensen, Christoffer Tyrsted, Martin Bremholm, Espen D. Bøjesen, Dipankar Saha, Steinar Birgisson, Mogens Christensen, Simon J. L. Billinge and Bo B. Iversen

Supporting information for

Towards atomistic understanding of polymorphism in solvothermal synthesis of ZrO_2 nanoparticles

Ann-Christin Dippel,[a,b] Kirsten M. Ø. Jensen,[c] Christoffer Tyrsted,[a] Martin Bremholm,[a] Espen D. Bøjesen,[a] Dipankar Saha,[a] Steinar Birgisson,[a] Mogens Christensen,[a] Simon J. L. Billinge,[c,d] Bo B. Iversen*[a]

[a] Center for Materials Crystallography, Department of Chemistry, Aarhus University, Langelandsgade 140, 8000 Aarhus C, Denmark

[b] Photon Science, Deutsches Elektronen-Synchrotron DESY, Notkestr. 85, 22607 Hamburg, Germany

[c] Applied Physics and Applied Mathematics, Columbia University, New York, New York 10027, USA

[d] Condensed Matter Physics and Materials Science Department, Brookhaven National Laboratory, Upton, New York 11973, USA

* Corresponding author: bo@chem.au.dk

Contents

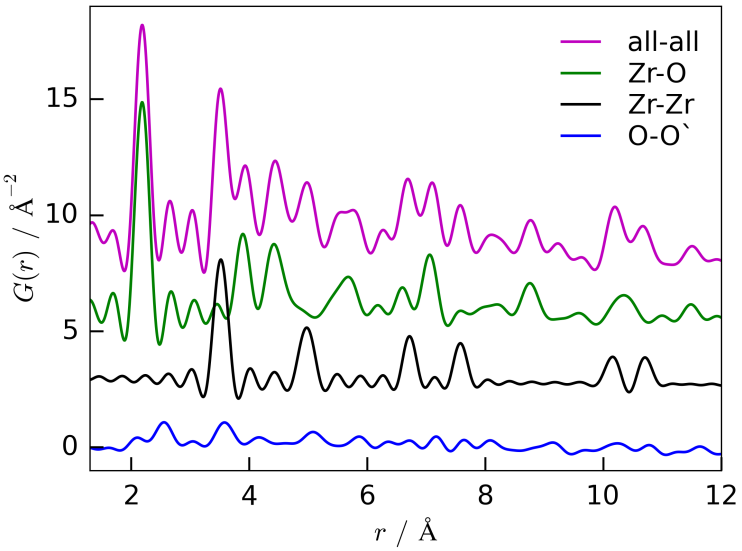

Figure S1: Partial PDFs calculated for the precursor structure in the program PDFgui[1] for the given atom pairs and Q_{max} = 16 Å^{-1}, Q_{damp} = 0.029 Å^{-1}.

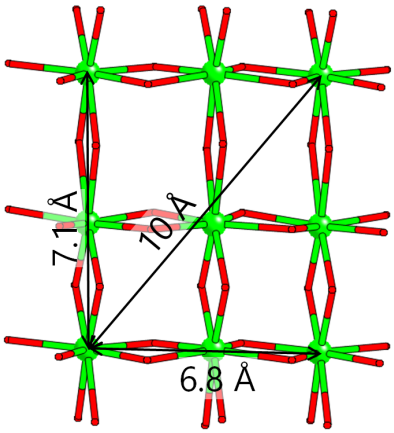

Figure S2. Schematic of the sheet structure proposed for zirconium compounds[2]; the intramolecular distances characteristic for the sheet structure of square-planar tetramers are indicated which are missing in the observed precursor structure for zirconium acetate in water and zirconium oxynitrate in methanol (see Fig. 2); zirconium ions are indicated by green spheres, red spheres for oxygen ions are omitted for clarity.

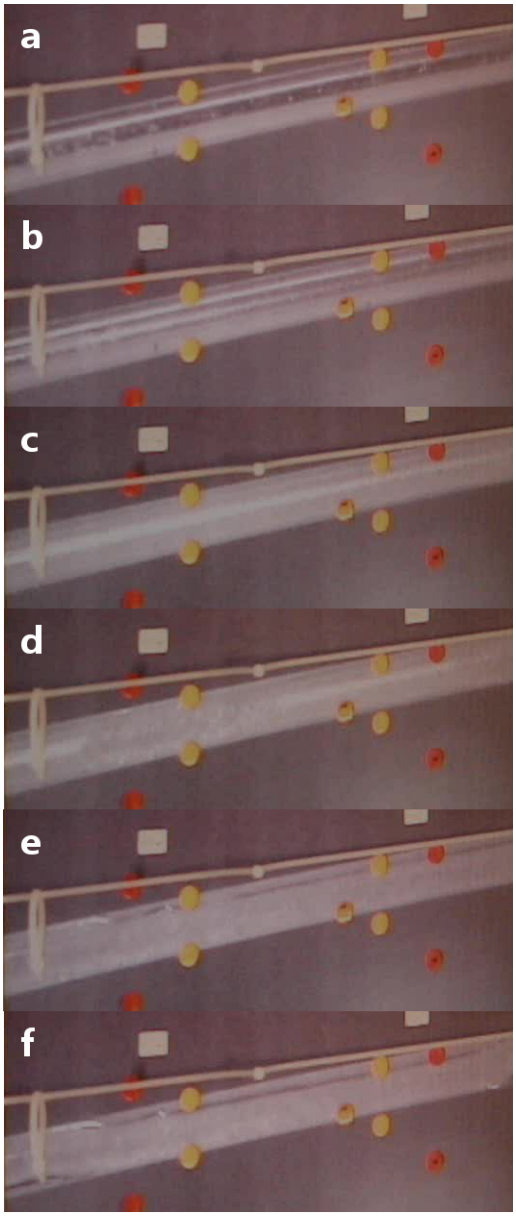

Figure S3: Sequence of selected frames from footage of the surveillance camera in the experimental hutch of beamline ID11 at the ESRF, showing the different stages during the solvothermal synthesis of ZrO_2 in the Ø 0.7 mm diameter capillary. These are in detail: a) precursor solution; b) formation of the intermediate; c) intermediate phase; d) break-up of the intermediate; e) dispersion of small ZrO_2 nanoparticles; f) dispersion of larger ZrO_2 nanoparticles. The yellow and red dots are artefacts from the recording.

Table S1. Parameters of the PDFgui[1] refinements of the crystalline phases as the end product of the synthesis after reaction times of 9.5 min for route H and 13.5 min for route M. The fit range was 1.3 – 40 Å. Parameters m1-9 and t1 are explained in Table S2. The uncertainties are based on the routine described in Ref. [3].

parameter	route M		route H	
	monoclinic	tetragonal	monoclinic	tetragonal
norm. scale factor	0.74 (1)	0.256(6)	0.907(8)	0.093(4)
diameter / Å	43.5(6)	46(1)	48.8(5)	58(3)
δ_2	2.8(3)	4.7(1)	3.0(2)	5.6(7)
a / Å	5.162(1)	3.644(1)	5.1741(8)	3.616(1)
b / Å	5.207(1)	3.644(1)	5.2252(8)	3.616(1)
c / Å	5.339(1)	5.081(3)	5.3497(7)	5.202(4)
β / °	99.41(2)	90	99.42(2)	90
m1 // t1	0.065(4)	0.738(6)	0.072(2)	0.798(3)
m2	0.155(4)		0.147(2)	
m3	0.833(4)		0.856(2)	
m4	0.397(6)		0.444(2)	
m5	0.789(4)		0.760(2)	
m6	0.957(3)		0.979(2)	
m7	0.2789(3)		0.2784(2)	
m8	0.4597(3)		0.4600(2)	
m9	0.7114(4)		0.7105(3)	
U_{iso} (Zr)	0.0038(1)	0.0100(4)	0.00533(9)	0.0087(6)
U_{iso} (O)	0.037(3)	0.056(4)	0.024(1)	0.016(3)
R_w	0.174		0.24	

Table S2. Refinement parameters for atomic coordinates based on symmetry constraints for the monoclinic and tetragonal phase.

	monoclinic			tetragonal		
Site	*x*	*y*	*z*	*x*	*y*	*z*
O1	m1	m2	m3	0	0.5	t1
O2	-m1 + 1	m2 + 0.5	-m3 + 1.5	0.5	0	-t1 + 1.5
O3	-m1 + 1	-m2 + 1	-m3 + 1	0.5	0	-t1 + 1
O4	m1	-m2 + 0.5	m3 – 0.5	0	0.5	t1 – 0.5
O5	m4	m5	m6			
O6	-m4 + 1	m5 – 0.5	-m6 + 1.5			
O7	-m4 + 1	-m5 + 1	-m6 + 1			
O8	m4	-m5 + 1.5	m6 – 0.5			
Zr1	m7	m8	m9	0.5	0.5	0.5
Zr2	-m7 + 1	m8 + 0.5	-m9 + 1.5	0	0	0
Zr3	-m7 + 1	-m8 + 1	-m9 + 1			
Zr4	m7	-m8 + 0.5	m9 – 0.5			

Table S3. Rietveld refinement parameters for the end products (same datasets as used for the refinements in real space shown in Table S1) of both routes M and H performed using MAUD.[4] Note that the measurement conditions were optimised for *in situ* PDF analysis, *i.e.* maximum Q range, so that the angular resolution is rather low. The background was modelled with two background peaks mixed with a 3rd order polynomial, and isotropic crystallite sizes based on integral breadths (Delft model) were chosen for the Rietveld refinement. Wavelengths were 0.190 Å in the case of route M and 0.207 Å for route H. Unit cell, zero shift, scale factor, and crystallite size were refined, while structural parameters (atomic positions, thermal displacement parameters) were kept at the values given by the CIF reference file. The results from real space and reciprocal space Rietveld refinements qualitatively agree in the observed trends, though the absolute values of scale factors and diameters deviate due to different weighing schemes and different size models.

parameter	route M		route H	
	monoclinic	tetragonal	monoclinic	tetragonal
a (Å)	5.177(3)	3.604(1)	5.167(2)	3.595(2)
b (Å)	5.215(3)	3.604(1)	5.223(2)	3.595(2)
c (Å)	5.334(3)	5.216(3)	5.341(2)	5.245(6)
β (°)	99.44(4)	90	99.51(3)	90
crystallite size (Å)	92(7)	86(12)	119(6)	90(9)
weight fraction (%)	61(2)	39(2)	85(2)	15(2)
global R_p	0.011	0.011	0.011	0.011
global R_{wp}	0.015	0.015	0.013	0.013

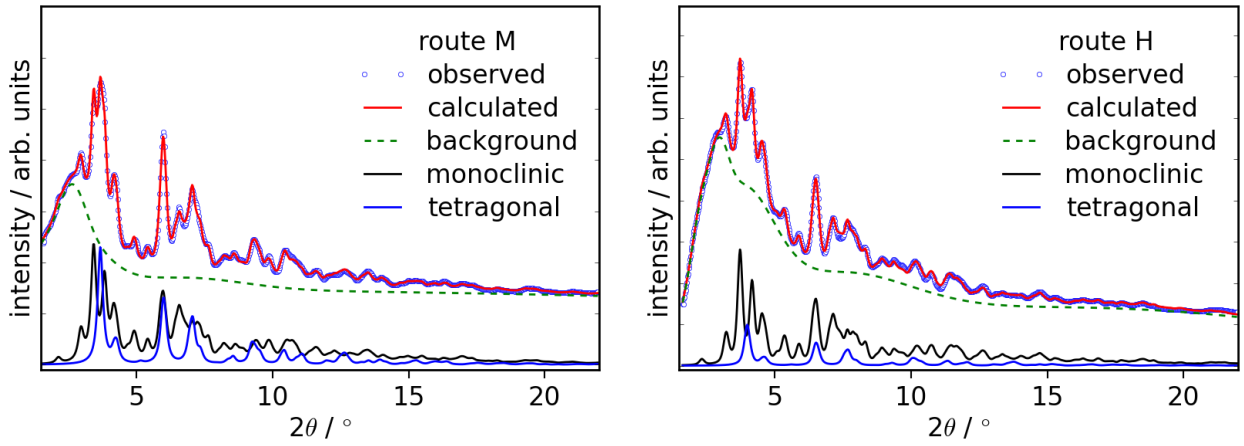

Figure S4. Graphic representation of the reciprocal space Rietveld refinements described in Table S3.

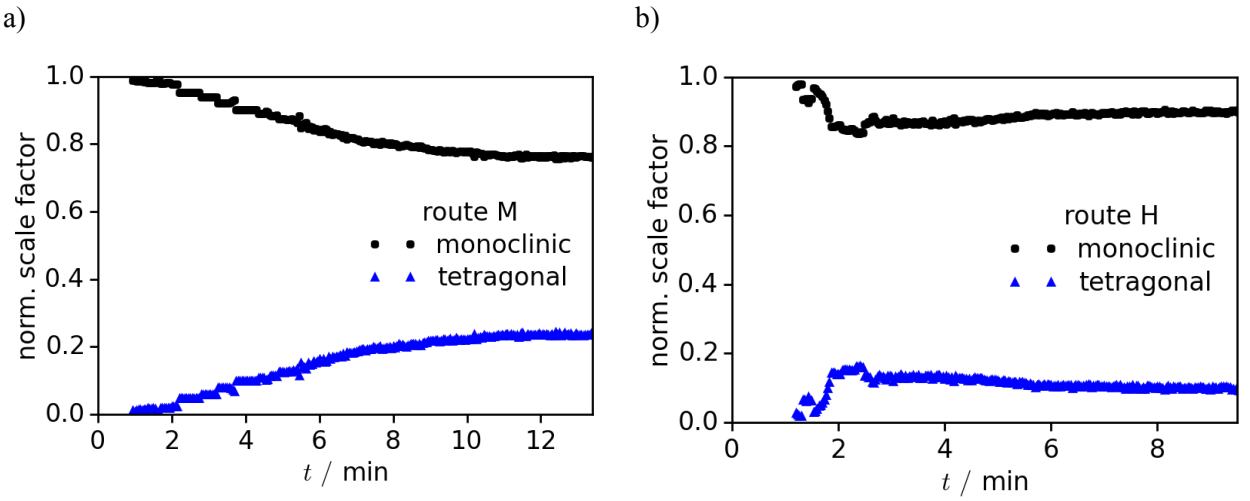

Figure S5. Evolution of scale factors (normalised to the interval 0-1) for the monoclinic (black circles) and the tetragonal (blue triangles) structures during nanoparticle formation in (a) route M and (b) route H. The values were obtained by sequential two-phase refinements in PDFgui[1] in reverse order, *i.e.* starting from the end product using the refined values given in Table S1 (r range 1.3 – 40 Å, fixed thermal displacement parameters) and refining frame by frame backwards to the beginning of the synthesis. The monoclinic scale factor starts at a value of 1 as the intermediate phase is modelled with local monoclinic order. These data do not suggest that there is a transformation from small tetragonal nuclei / crystallites into monoclinic crystallites at a critical size limit.

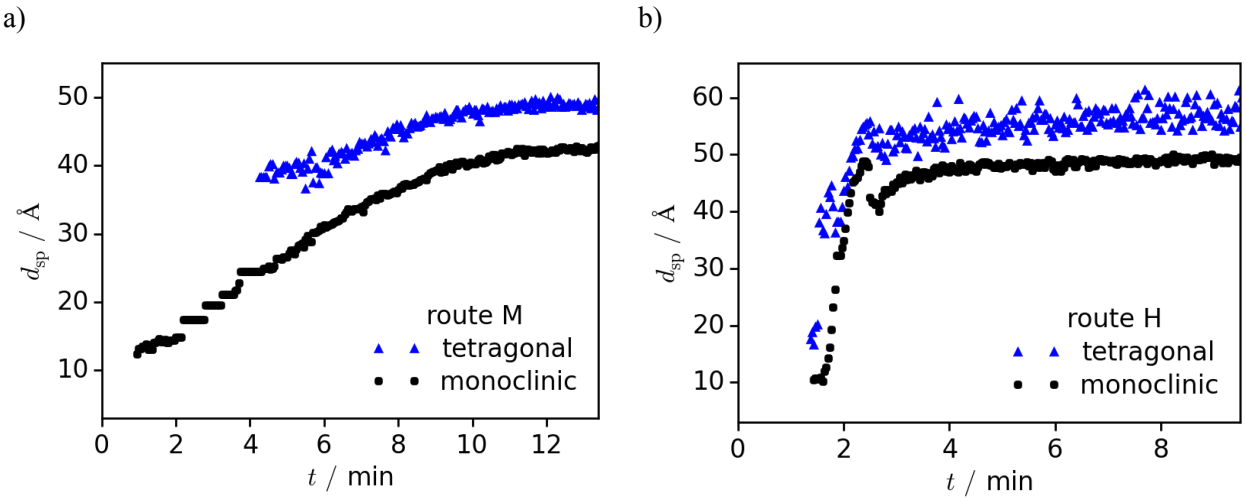

Figure S6. Growth curves for the two routes M (a) and H (b) in terms of the spherical particle diameter from the real space Rietveld refinement in PDFgui[1] for the monoclinic (black circles) and the tetragonal (blue triangles) phase. In route M, the refinement of the smaller particles sizes of the tetragonal phase (scale factor below ~ 0.1) was attributed with a large error making the values physically insignificant, hence these data are omitted in the plot.

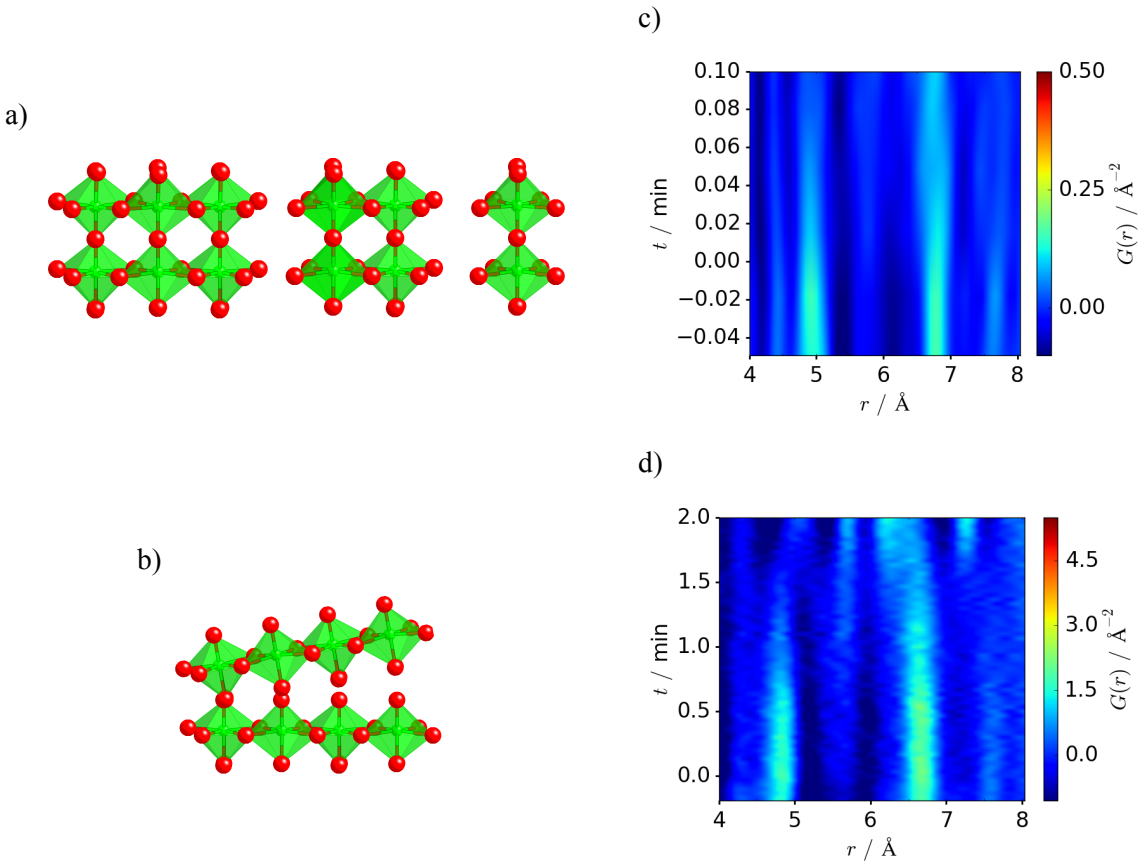

Figure S7. Schematic break-up scenarios of the precursor chain structure a) across and b) along the chain axis. In case a), the tetrameric motif (PDF peak at ~5 Å) survives longer than the buckled chain (PDF peak at 6.8 Å), and vice-versa for case b). Zoom into the *in situ* PDF series for c) route M and d) route H to illustrate the break-up sequence of the medium range order for both cases. In route M, both PDF peaks lose intensity on the same time scale, whereas in route H, the PDF peak corresponding to the buckled chain motif persist longer, suggesting that the break-up mechanism b) dominates.

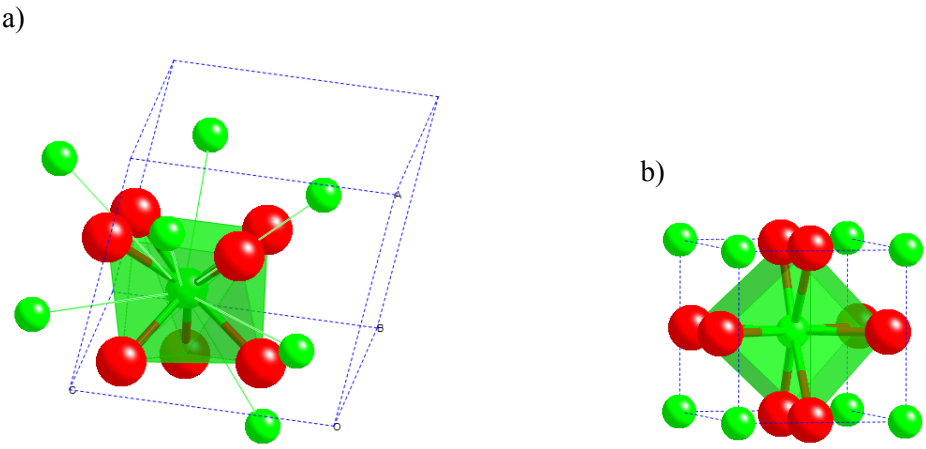

Figure S8. Local ordering around Zr in the monoclinic (a) and the tetragonal (b) phase, represented by the first two coordination shells of Zr-O and Zr-Zr bonds, along with the respective unit cell. As a guide to the eye for the steric orientation of the outer Zr atoms, the Zr-Zr correlations are marked by green lines in the complex monoclinic structure, which is not to be mistaken as an actual chemical bond.

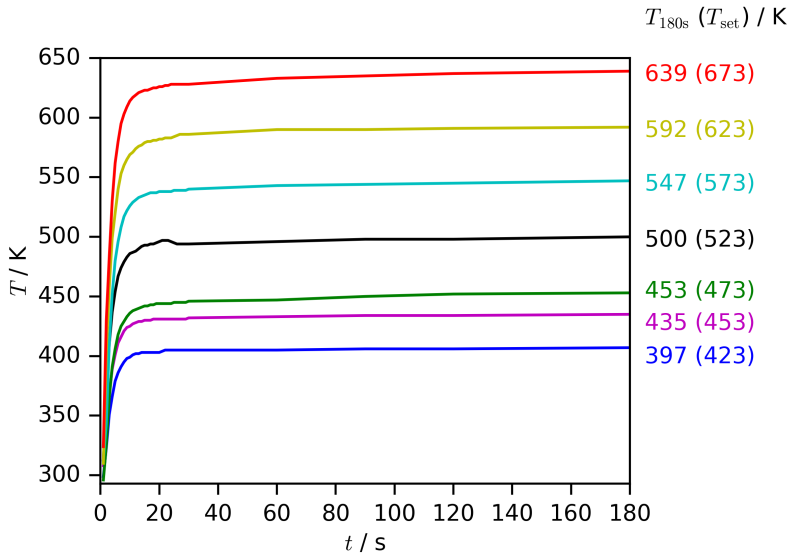

Figure S9. Temperature profiles of the *in situ* reactor determined by means of a thermocouple located at the sample position (after Ref. [5]). T_{set} refers to the set temperature at the temperature controller. For routes M and H, T_{set} was 275 and 230 °C, respectively. The temperature values used in the manuscript are extrapolated from the measured values.

References

[1] A. Clearfield, *J. Mater. Res.* **1990**, 5, 161-162.

[2] C. L. Farrow, P. Juhas, J. W. Liu, D. Bryndin, E. S. Božin, J. Bloch, T. Proffen, S. J. L. Billinge, *J. Phys.: Condens. Matter* **2007**, 19, 335219.

[3] K. M. Ø. Jensen, M. Christensen, P. Juhás, C. Tyrsted, E. D. Bøjesen, N. Lock, S. J. L. Billinge, B. B. Iversen, *J. Amer. Chem. Soc.*, **2012**, 134, 6785-6792.

[4] L. Lutterotti, S. Matthies, H. -R. Wenk, Proceeding of the Twelfth International Conference on Textures of Materials (ICOTOM-12) **1999**, 1, 1599-1604.

[5] E. D. Bøjesen, K. M. Ø. Jensen, C. Tyrsted, N. Lock, M. Christensen, B. B. Iversen, Cryst. Growth Des. **2014**, 14, 2803-2810.